IEEE Access
Multidisciplinary ⋮ Rapid Review ⋮ Open Access Journal

Received January 9, 2022, accepted March 27, 2022, date of publication April 6, 2022, date of current version May 3, 2022.

Digital Object Identifier 10.1109/ACCESS.2022.3165428

A Hybrid Fabrication Technique of Capacitive Flow Meters Using Three-Dimensional Printing for Rectifying Airflows

SANGHUN SHIN[1], GAHUI PARK[2], WHOI-YUL KIM[2], (Member, IEEE), AND HONGYUN SO[1,3], (Member, IEEE)

[1]Department of Mechanical Engineering, Hanyang University, Seoul 04763, South Korea
[2]Department of Electronics and Computer Engineering, Hanyang University, Seoul 04763, South Korea
[3]Institute of Nano Science and Technology, Hanyang University, Seoul 04763, South Korea

Corresponding author: Hongyun So (hyso@hanyang.ac.kr)

This work was supported by the National Research Foundation of Korea (NRF) by the Ministry of Science and ICT of the Republic of Korea under Grant NRF-2020R1A4A1019074.

ABSTRACT In this study, a simple manufacturing method was developed for fabricating a multifunctional capacitive flow meter (CFM), which can act as a check valve for flow channels. By using three-dimensional (3D) printing technology, a hybrid advanced manufacturing process is realized. As the gas flows in the forward direction, the initially closed polymer membrane opens and allows airflow. The flexible and dielectric membrane is normally closed. It opens in response to the airflow direction and changes the capacitance according to the airflow rate. The sensing performance of four different CFMs were characterized according to the thickness of the membrane. From an analysis of the static and transient responses, the sensing range, sensitivity, and signal-to-noise ratio were calculated and compared. The CFM with a 600 μm thick membrane was adopted as the sensing component for a human respiratory (inhalation and exhalation) monitoring system as one of the applications. The 3D printed system successfully measured the respiratory rate and tidal volume ($\sim$442.3 ml), supporting the applicability of CFMs in diverse fields such as human healthcare, mass flow controllers, and smart wearable devices.

INDEX TERMS Capacitive sensor, 3D printing, flow meter, respiratory healthcare, check valve.

I. INTRODUCTION

In the past few decades, precise flow rate measurement has been crucial not only in industrial fields such as the oil and gas industries, but also for human respiratory healthcare fields [1]–[4]. Therefore, selecting the appropriate type of flow meter is also important by considering the sensitivity and sensing range requirements of the application. To meet this demand, several different micromachined flow sensors have been widely studied, such as thermal [2], [5], [6] and non-thermal types [3]–[5]. The principle of the thermal type is based mainly on the asymmetric temperature distribution of the heating component by convective heat dissipation during fluid or gas flow [2], [7]. However, because the presence of the high temperature element has potential risks of fire for combustible gas measurements, additional monitoring systems are required.

For the other non-thermal flow sensors including piezoresistive [8], [9] and capacitive [3], [4], [10] types, issues such as sensitivity, sensing range, and temperature dependency need to be improved. Moreover, the traditional microelectromechanical system (MEMS)-based fabrication processes require complex fabrication (such as photolithography, metal deposition, and etching) and extremely clean facilities. These constraints have entailed high costs for mass-production manufacturing for widespread applications. As a result, a simple and low-cost flow sensor fabrication is required.

Recently, three-dimensional (3D) printing technology has been considered as an innovative solution for smart manufacturing fields, owing to the convenient and intuitive methods used. The previous complicated fabrications for microscale devices such as microfluidic chips, sensors, and actuators, have been replaced with 3D printing-assisted methods for

The associate editor coordinating the review of this manuscript and approving it for publication was Xiaokang Yin.

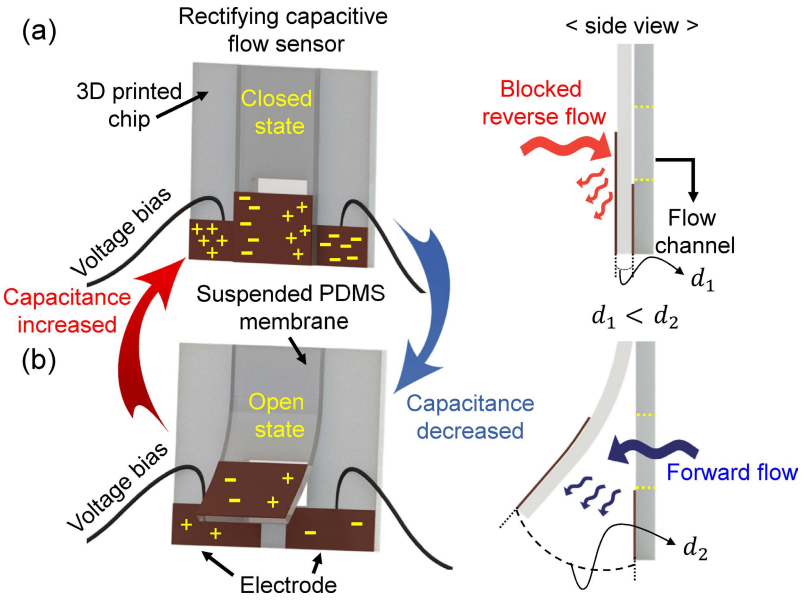

FIGURE 1. Conceptual schematic of a 3D printing-assisted capacitive flow rate sensor and the sensing principle for different flow directions: (a) backward (red), and (b) forward (blue).

several different practical applications such as human healthcare [11]–[13], constructing structures [14]–[16], and electrical components [17]–[19]. In particular, owing to the printing capability of biocompatible filaments, there have been many efforts made to develop 3D printed biomedical devices such as artificial organs [11], [20], electronic skins [12], [21], and wearable devices [13], [22] for the human healthcare industry. Moreover, by substituting traditional MEMS fabrication, various printing processes have been adopted to develop various sensing devices. For instance, force [23], strain [24], and humidity sensors[25] were directly printed, realizing a facile and cost-effective fabrication. Consequently, the precise characterization of products using both experimental and theoretical methods is important.

Capacitance-based devices are frequently used owing to their high stability and short response time [26], [27]. As the capacitance is related to the relative permittivity, distance between electrodes, and their area, capacitive pressure sensors have been widely fabricated using sandwich structures [26]–[28]. In addition, multiphase flow [29]–[31] and liquid level [32]–[34] detections were performed by measuring the capacitance change in response to the mean dielectric property between two electrodes by the variation of volume fraction and the amount of liquid, respectively.

In this study, we developed a 3D printing-assisted simple and low-cost method to fabricate a capacitive flow meter (CFM) using a suspended dielectric membrane. Figure 1 illustrates the overall principle of the CFM for forward and reverse flows. The two copper electrodes were fixed on the 3D printed chip with a gap for voltage bias, and additional electrodes were initially placed above them without electrical contact because of the thickness of the suspended polymer film (d_1). As shown in Fig. 1(a), the suspended polydimethylsiloxane (PDMS) membrane remains in a fully closed state when the fluid flows in the reverse direction or there is no flow. Because of its structural properties, the flow is blocked by the membrane and cannot pass through the flow channel. In contrast, the suspended PDMS membrane naturally opens when the fluid flows forward, and the distance between the attached and suspended electrodes increases (from d_1 to d_2). As the amount of charge initially collected at the attached electrodes decreases, the output capacitance also decreases. As a result, continuous flow rate measurement is achieved because the decreased rate of the capacitance is directly related to the flow rate. Moreover, as the flow sensor can be used as a check valve for the flow channel, it can detect gas flow in a specific direction. In addition, the CFMs can be utilized for potential applications such as drug delivery, exhalation monitoring systems, and hemodialysis machines by connecting in series within the fluid channel to measure the forward flow rate selectively. To characterize the capacitive flow sensor according to the different thicknesses of the polymer membrane, both static and transient analyses were conducted using the experimental method in response to the flow rate. In addition, the sensing performance trends were evaluated to determine the sensing range and sensitivity. Finally, to demonstrate the flow rectifying characteristics, capacitive flow sensors were applied to a human respiratory (exhalation and inhalation) monitoring device to calculate the respiratory rate and tidal volume. This study demonstrated the simple fabrication and analysis of flow sensors with wide sensing ranges for different applications, such as respiratory detection and gas flow meters.

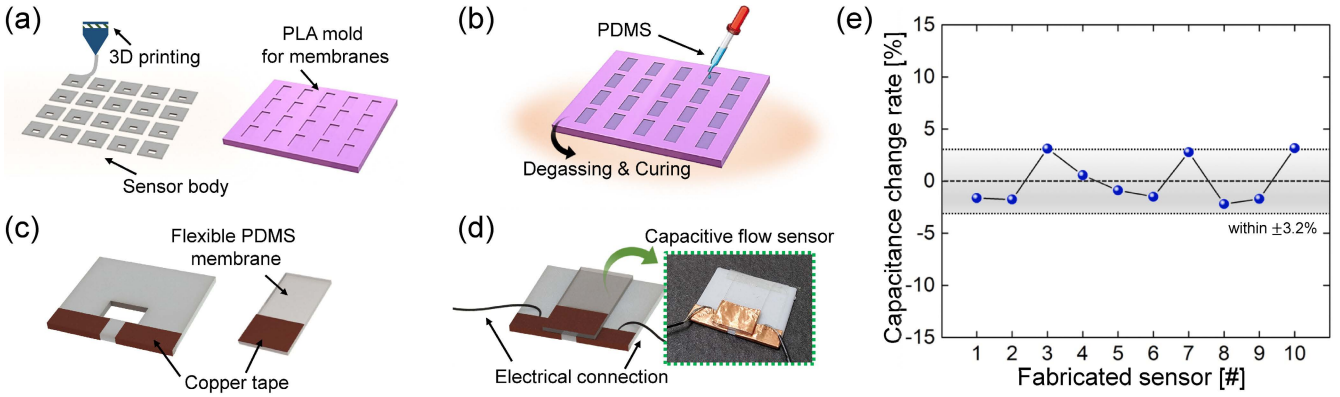

FIGURE 2. Overall fabrication process of the CFM: (a) 3D printing process for sensor body and mold for PDMS membrane; (b) PDMS pouring, degassing, and curing processes for different thicknesses; (c) combining copper tape with sensor body and PDMS membrane; (d) integration of the two parts and electrical connection for the capacitive sensing; and (e) comparison of initial capacitance of ten fabricated CFMs (membrane thickness = 900 μm).

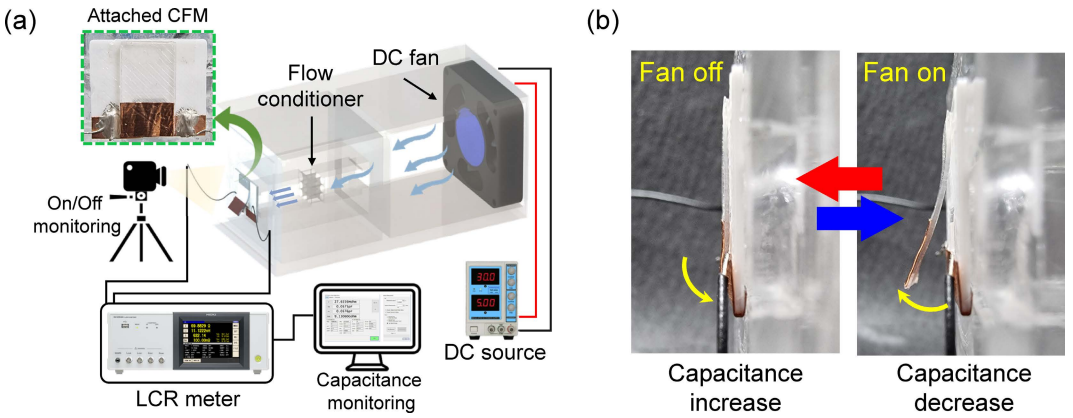

FIGURE 3. (a) Schematic configuration of experimental setup to characterize fabricated CFMs. (b) Movement of a suspended PDMS membrane during fan on/off.

II. FABRICATION

As depicted in Fig. 2, the fabrication process for CFMs consists of four main steps: 3D printing of the main body and mold, PDMS membrane curing, electrode formation, and assembly with wire connections. Figure 2(a) shows the printing of the sensor bodies and mold of the PDMS membranes. For the sensor bodies containing a 5 mm × 2.5 mm rectangular hole, fused deposition modeling-based 3D printing (Guider IIs, Zhejiang Flashforge 3D Technology co., Ltd.) was used with a polylactic acid (PLA) filament. At the same time, a 3D printer (3DWOX 2X, Sindoh Co., Ltd.) with a nozzle diameter of 0.4 mm was used for printing PLA filaments to prepare the membrane mold. The printing speed, filling density, bed temperature, nozzle temperature, and layer thickness were selected as 40 mm/s, 100%, 50 °C, 210 °C, and 0.15 mm, respectively. Subsequently, the degassed PDMS polymer mixture (ratio of prepolymer to curing agent = 10:1) was poured into the printed membrane mold and kept for 24 h at room temperature, as shown in Fig. 2(b). PDMS membranes were fabricated with four different thicknesses of 300, 600, 900, and 1200 μm (hereinafter referred to as 3-, 6-, 9-, and 12-type, respectively) and fixed width and length (7.35 and 13 mm, respectively) to compare the sensing performances. The thickness of the polymer films can be easily controlled by the 3D printing method. Subsequently, ∼0.05 mm thickness of copper tape was cut into 5 mm × 7 mm, to create bottom electrodes on the sensor body, and top electrodes on the flexible PDMS membrane, as illustrated in Fig. 2(c). Specifically, to generate capacitance, the two bottom electrodes were attached with a gap of 2 mm. Finally, the sensor body and membrane were assembled to complete the fabrication process, and the copper wires were connected for external electrical access, as shown in Fig. 2(d). The three electrodes do not touch each other owing to the polymer membrane separating them during both forward and reverse flows. Furthermore, to evaluate the effect of non-flat copper tape due to manual processes on capacitance, the initial capacitance at closed state were analyzed with ten fabricated sensors. As a result, the CFMs exhibited the average capacitance of ∼0.35 pF within ±3.2% deviation, as shown in Fig. 2(e), demonstrating the negligible effect of the uneven surface of copper tape and reliable fabrication results.

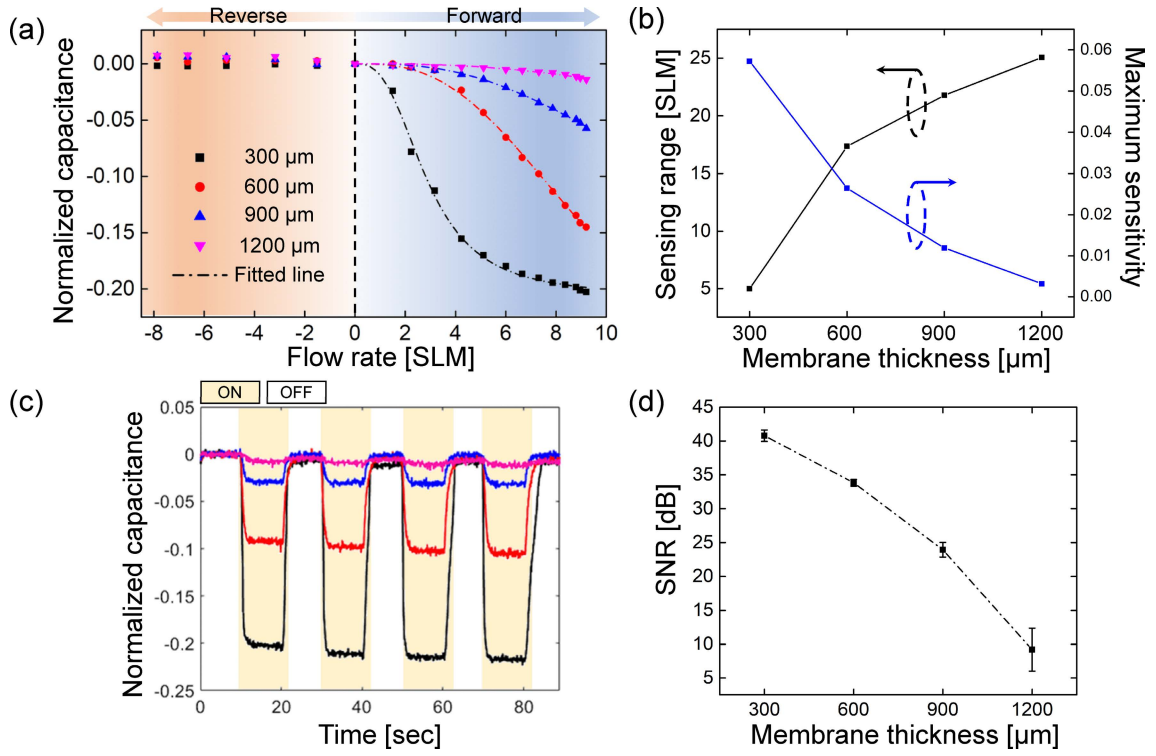

FIGURE 4. Sensing performance comparison of the fabricated flow sensors with different membrane thicknesses: (a) normalized capacitance as a function of flow rate, (b) effective sensing range and maximum sensitivity as a function of membrane thickness, (c) transient response for 10 s cyclic flows at 7.87 SLM, and (d) signal-to-noise ratio as a function of membrane thickness.

III. CHARACTERIZATION

To characterize the sensing performance of the CFMs with respect to the flow rate and thickness of the polymer membrane, the sensor was attached to a testbed, as shown in Fig. 3(a). In addition, to evaluate capacitance change at reverse flow conditions, CFMs were attached to the inlet of flow channel. A DC controllable fan was used to supply a continuous airflow rate by changing the DC voltage input through a regulated power supply (TDP-305A, TOYOTech LLC). It should be noted that before the fluid reached the sensor, the flow profile was regulated uniformly using a flow conditioner. In addition, to determine the correlation between the input DC voltage and flow rate, a commercial flow meter (PMF4005V, POSIFA Microsystems, Inc.) was attached to the outlet of the testbed. Subsequently, the change in the capacitance of the fabricated sensing device fixed at the same position was measured using an LCR meter (IM3536, HIOKI E.E. Corporation). For the measurement, the AC frequency, AC voltage, and DC voltage were set to 100 kHz, 2 V, and 1 V, respectively. Simultaneously, optical images were captured to qualitatively detect membrane movement during the tests. Figure 3(b) shows the behavior of the polymer membrane in response to the flow direction. The gap between the electrodes increases as the membrane opens when the flow rate increases (fan on), thereby decreasing the capacitance, as compared with the initial state (fan off) or when the fluid flows in the reverse direction.

IV. RESULTS AND DISCUSSION

Figure 4(a) shows the average sensing performance results of the four different 3-, 6-, 9-, and 12-type CFMs as a function of the supplied flow rate. For each measurement, the capacitance was measured for each flow rate condition in the range of ∼-7.9 to ∼9.2 SLM (standard L/min). The evaluated capacitance was normalized based on the initial value for each experiment to compare the results. The equation for normalization is calculated as follows:

$$C_{normalized} = (C_d - C_i)/C_i \tag{1}$$

where C_i is the initial capacitance without flows and C_d is the value decreased by the airflows. Note that ∼0.34, ∼0.37, ∼0.35, and ∼0.41 pF were measured for the average initial capacitance value of 3-, 6-, 9-, and 12-type CFMs, respectively. As seen in Fig. 4(a), although the PDMS membrane could be slightly deformed by the negative pressure (i.e., reverse flow), capacitance changed less than ∼0.8%, which was negligible compared to the initial value. As a result, it should be noted that the CFMs could successfully rectify the reverse flow without considerable noise. For the forward flow conditions, the thinner the polymer film, the greater the sensitivity in the relatively low flow rate region (0−4 SLM). In addition, for the 3-type CFMs (3-CFMs), the changed capacitance rate converged (i.e., low effective sensing range) in the relatively high flow rate region (7−9.2 SLM). For the 12-CFMs, the overall sensitivity is low

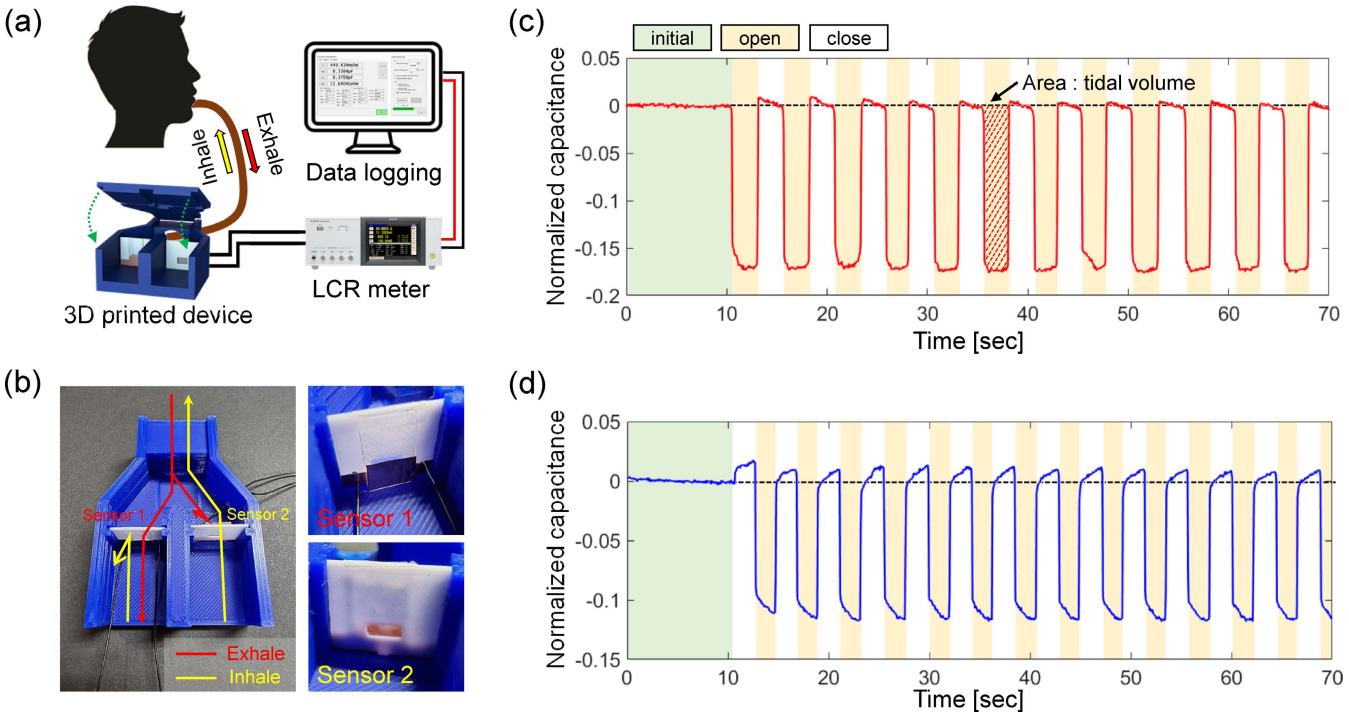

FIGURE 5. (a) Configuration of respiratory monitoring system using fabricated CFMs and a 3D printed case. (b) Mounted CFMs for the independent sensing of exhalation (red line) and inhalation (yellow line). Transient sensing response for (c) exhalation, and (d) inhalation.

in the given flow range compared with the other CFM types because more force is required to lift the membrane, however, an effective sensing region exists at a higher flow rate. Furthermore, because there was a limitation to the distance that the polymer films could be lifted, it can be seen that the rate of change was saturated at the higher flow rates. It was noticeable that the overall level of capacitance and sensitivity can be easily enhanced by utilizing other dielectric materials and tuning the gap between sensing electrodes.

Moreover, for the continuous measurement of the forward flow rate and to analyze the range of the effective sensing region and sensitivity for reliable future applications, a nonlinear curve fitting was adjusted using a logistic function [35], [36] (dotted line) considering the characteristics of the results. The equation used for fitting can be described as

$$C_{normalized} = \alpha(1 - \frac{1}{1 + (x/x_0)^{2.8}}) \tag{2}$$

where x is the flow rate, and the other parameters (α and x_0) are fitting constants. The fitted curves matched well with R-squared values of 0.997, 0.998, 0.997, and 0.957 for the 3-, 6-, 9-, and 12-type CFMs, respectively. Because the slope of the curve represents the sensitivity, the maximum sensitivity and effective sensing range (difference in flow rate between 10% and 90% of the initial and converged capacitance values) can be easily calculated by differentiating the fitted functions. Figure 4(b) shows a comparison of the sensing performance as a function of the membrane thickness. For the intuitive comparison, absolute value was used for the sensitivity calculation. As the thickness of the polymer membrane increased, although the maximum sensitivity decreased (0.057 to 0.003 1/SLM for 3- to 12-CFM, respectively), the effective sensing range increased (4.99 to 25.06 SLM for 3- to 12-CFM, respectively). It should be noted that by tuning the thickness of the polymer membrane, the appropriate type of CFM can be selected for each required specification.

Figure 4(c) exhibits transient responses with a periodic fan on/off condition for the four different CFM types. Each condition applied to the sensing components lasted 10 s with a flow rate of ∼7.87 SLM when the fan was on. As a result, the sensitivity of the thinner type of CFM shows enhanced sensitivity under repeated flow rates. In addition, the average signal-to-noise ratio (SNR_{dB}) values were calculated, where $SNR_{dB} = 20\log_{10}(C_{signal}/C_{noise})$, to compare the signal discrimination performance. As depicted in Fig. 4(d), the noise generated from the capacitance signal is negligible for the 3-, 6-, and 9-CFM owing to their high SNR_{dB} values > 20. However, the 12-CFM showed a relatively low SNR_{dB} (∼9.2) and a high standard deviation. In summary, for reliable and stable sensing results, a CFM with less than a 1200 μm polymer membrane thickness is desirable.

To demonstrate CFMs as respiratory monitoring sensors for digital health applications, the sensing performance in human breathing was observed using an additional 3D printed case. Because the 6-CFMs exhibit relatively high sensitivity (0.026 1/SLM), an effective sensing range (17.36 SLM), and SNR_{dB} (33.85 dB), PDMS membranes with 600 μm thickness were selected for the respiratory measuring components.

Figure 5(a) shows an overall schematic of the respiratory monitoring system using CFMs. The device was designed to have two breathing flows (inhale and exhale) with two channels by mounting the two CFMs in opposite configurations, to detect the reverse direction of each flow (sensor 1 and 2 for exhalation and inhalation, respectively). Because the CFMs can rectify fluid flows (blocking reverse flow), complete exhalation or inhalation can be achieved with the intended sensor without additional check valves. For instance, while inhaling (yellow line in Fig. 5(b)), sensor 1 is naturally closed, and the fluid flows only through sensor 2, such that the inspiratory flow can be measured. By sealing the fabricated device, a human respiratory monitoring system can be realized using an LCR meter. Exhalation and inhalation of breath were successfully detected for 70 s as depicted in Figs. 5(c) and 5(d), respectively. To demonstrate the reliable sensing performance of the system, the respiratory rate and average tidal volume were measured by calculating the breaths per minute and the average area during exhalation, respectively. As a result, the device measured the parameters as ∼13 breaths/min and ∼442.3 mL of tidal volume, which was comparable to the normal range for adults [37], [38]. Therefore, these results demonstrate the reliable application of CFMs in human respiratory healthcare.

V. CONCLUSION

In conclusion, a simple method of 3D printing-based fabrication of a CFM was proposed for a human respiratory monitoring device. Owing to the suspended polymer membrane with a dielectric layer, the CFMs can measure flow rates and rectify the reverse flow simultaneously. The airflow rate sensing performance was compared for different PDMS thicknesses (300, 600, 900, and 1200 μm) by static and transient analyses. In addition, the results were fitted with a logistic curve to compare the effective sensing range and sensitivity. Furthermore, using repeated transient tests, the SNR_{dB} was evaluated. Evaluating the optimal mix of sensitivity, effective flow sensing range and SNR_{dB}, CFMs with 600 μm thick membranes were selected for demonstration of human healthcare applications. To realize the respiratory monitoring system, an additional 3D printed package was used to fix two 6-CFMs for independent sensing of inhalation and exhalation. A respiratory rate of ∼13 breaths/min and ∼442.3 mL of tidal volume were successfully measured within a reasonable range. These results support the novel manufacturing method for controllable capacitive flow rate measuring devices and human respiratory monitoring systems by using static and transient analysis of the flow sensor.

REFERENCES

[1] X. Shi, C. Tan, F. Dong, and J. Escudero, "Flow rate measurement of oil-gas-water wavy flow through a combined electrical and ultrasonic sensor," *Chem. Eng. J.*, vol. 427, Jan. 2022, Art. no. 131982.
[2] N. A. Djuzhev, V. T. Ryabov, G. D. Demin, M. A. Makhiboroda, I. D. Evsikov, M. M. Pozdnyakov, and V. A. Bespalov, "Measurement system for wide-range flow evaluation and thermal characterization of MEMS-based thermoresistive flow-rate sensors," *Sens. Actuators A, Phys.*, vol. 330, Oct. 2021, Art. no. 112832.
[3] S.-H. Liao, W.-J. Chen, and M. S.-C. Lu, "A CMOS MEMS capacitive flow sensor for respiratory monitoring," *IEEE Sensors J.*, vol. 13, no. 5, pp. 1401–1402, May 2013.
[4] Z. Guo, T. Zhang, F. Zhou, and F. Yu, "Design and experiments for a kind of capacitive type sensor measuring air flow and pressure differential," *IEEE Access*, vol. 7, pp. 108980–108989, 2019.
[5] N. T. Nguyen, "Micromachined flow sensors—A review," *Flow Meas. Instrum.*, vol. 8, no. 1, pp. 7–16, Mar. 1997.
[6] T. S. Leu, J. M. Yu, J. J. Miau, and S. J. Chen, "MEMS flexible thermal flow sensors for measurement of unsteady flow above a pitching wind turbine blade," *Exp. Thermal Fluid Sci.*, vol. 77, pp. 167–178, Oct. 2016.
[7] T. H. Kim, D.-K. Kim, and S. J. Kim, "Study of the sensitivity of a thermal flow sensor," *Int. J. Heat Mass Transf.*, vol. 52, nos. 7–8, pp. 2140–2144, Mar. 2009.
[8] S. Abolpour Moshizi, H. Moradi, S. Wu, Z. J. Han, A. Razmjou, and M. Asadnia, "Biomimetic ultraflexible piezoresistive flow sensor based on graphene nanosheets and PVA hydrogel," *Adv. Mater. Technol.*, vol. 7, no. 1, Sep. 2021, Art. no. 2100783.
[9] Q. Zhang, W. Ruan, H. Wang, Y. Zhou, Z. Wang, and L. Liu, "A self-bended piezoresistive microcantilever flow sensor for low flow rate measurement," *Sens. Actuators A, Phys.*, vol. 158, no. 2, pp. 273–279, 2010.
[10] G. J. M. Krijnen, M. Dijkstra, J. J. V. Baar, S. S. Shankar, W. J. Kuipers, R. J. H. D. Boer, D. Altpeter, T. S. J. Lammerink, and R. Wiegerink, "MEMS based hair flow-sensors as model systems for acoustic perception studies," *Nanotechnology*, vol. 17, no. 4, pp. S84–S89, Feb. 2006.
[11] J. Li, Y. Long, F. Yang, H. Wei, and Z. Zhang, "Multifunctional artificial artery from direct 3D printing with built-in ferroelectricity and tissue-matching modulus for real-time sensing and occlusion monitoring," *Adv. Funct. Mater.*, vol. 30, no. 39, Sep. 2020, Art. no. 2002868.
[12] P. Wei, X. Yang, Z. Cao, X. Guo, H. Jiang, Y. Chen, M. Morikado, X. Qiu, and D. Yu, "Flexible and stretchable electronic skin with high durability and shock resistance via embedded 3D printing technology for human activity monitoring and personal healthcare," *Adv. Mater. Technol.*, vol. 4, no. 9, Sep. 2019, Art. no. 1900315.
[13] A. Kalkal, S. Kumar, P. Kumar, R. Pradhan, M. Willander, G. Packirisamy, S. Kumar, and B. D. Malhotra, "Recent advances in 3D printing technologies for wearable (bio)sensors," *Additive Manuf.*, vol. 46, Oct. 2021, Art. no. 102088.
[14] Z. Zuo, J. Gong, Y. Huang, Y. Zhan, M. Gong, and L. Zhang, "Experimental research on transition from scale 3D printing to full-size printing in construction," *Construct. Building Mater.*, vol. 208, pp. 350–360, May 2019.
[15] Y. Zhang and F. Aslani, "Development of fibre reinforced engineered cementitious composite using polyvinyl alcohol fibre and activated carbon powder for 3D concrete printing," *Construct. Building Mater.*, vol. 303, Oct. 2021, Art. no. 124453.
[16] A. Kazemian and B. Khoshnevis, "Real-time extrusion quality monitoring techniques for construction 3D printing," *Construct. Building Mater.*, vol. 303, Oct. 2021, Art. no. 124520.
[17] W. Ye, W. Wu, X. Hu, G. Lin, J. Guo, H. Qu, and J. Zhao, "3D printing of carbon nanotubes reinforced thermoplastic polyimide composites with controllable mechanical and electrical performance," *Compos. Sci. Technol.*, vol. 182, Sep. 2019, Art. no. 107671.
[18] S. Shin and H. So, "Time-dependent motion of 3D-printed soft thermal actuators for switch application in electric circuits," *Additive Manuf.*, vol. 39, Mar. 2021, Art. no. 101893.
[19] P. F. Flowers, C. Reyes, S. Ye, M. J. Kim, and B. J. Wiley, "3D printing electronic components and circuits with conductive thermoplastic filament," *Additive Manuf.*, vol. 18, pp. 156–163, Dec. 2017.
[20] K. Wang, C.-C. Ho, C. Zhang, and B. Wang, "A review on the 3D printing of functional structures for medical phantoms and regenerated tissue and organ applications," *Engineering*, vol. 3, no. 5, pp. 653–662, Oct. 2017.
[21] T. Xia, R. Yu, J. Yuan, C. Yi, L. Ma, and F. Liu, "Ultrahigh sensitivity flexible pressure sensors based on 3D-printed hollow microstructures for electronic skins," *Adv. Mater. Technol.*, vol. 6, no. 3, Mar. 2021, Art. no. 2000984.
[22] Y. Tong, Z. Feng, J. Kim, J. L. Robertson, X. Jia, and B. N. Johnson, "3D printed stretchable triboelectric nanogenerator fibers and devices," *Nano Energy*, vol. 75, Sep. 2020, Art. no. 104973.
[23] M. Saari, B. Xia, B. Cox, P. S. Krueger, A. L. Cohen, and E. Richer, "Fabrication and analysis of a composite 3D printed capacitive force sensor," *3D Printing Additive Manuf.*, vol. 3, no. 3, pp. 136–141, Sep. 2016.
[24] G. L. Goh, S. Agarwala, and W. Y. Yeong, "3D printing of microfluidic sensor for soft robots: A preliminary study in design and fabrication," in *Proc. Int. Conf. Prog. Additive Manuf. (Pro-AM)*, vol. 2016, pp. 177–181.

[25] A. S. G. Reddy, B. B. Narakathu, M. Z. Atashbar, M. Rebros, E. Rebrosova, and M. K. Joyce, "Fully printed flexible humidity sensor," *Proc. Eng.*, vol. 25, pp. 120–123, Sep. 2011.
[26] Z. He, W. Chen, B. Liang, C. Liu, L. Yang, D. Lu, Z. Mo, H. Zhu, Z. Tang, and X. Gui, "Capacitive pressure sensor with high sensitivity and fast response to dynamic interaction based on graphene and porous nylon networks," *ACS Appl. Mater. Interface*, vol. 10, no. 15, pp. 12816–12823, Apr. 2018.
[27] L. Ma, X. Yu, Y. Yang, Y. Hu, X. Zhang, H. Li, X. Ouyang, P. Zhu, R. Sun, and C.-P. Wong, "Highly sensitive flexible capacitive pressure sensor with a broad linear response range and finite element analysis of micro-array electrode," *J. Materiomics*, vol. 6, no. 2, pp. 321–329, Jun. 2020.
[28] Z. Zhang, X. Gui, Q. Hu, L. Yang, R. Yang, B. Huang, B. Yang, and Z. Tang, "Highly sensitive capacitive pressure sensor based on a micropyramid array for health and motion monitoring," *Adv. Electron. Mater.*, vol. 7, no. 7, Jul. 2021, Art. no. 2100174.
[29] R. K. Rasel, B. Straiton, Q. Marashdeh, and F. L. Teixeira, "Toward water volume fraction calculation in multiphase flows using electrical capacitance tomography sensors," *IEEE Sensors J.*, vol. 21, no. 6, pp. 7702–7712, Mar. 2021.
[30] C. N. Strizzolo and J. Converti, "Capacitance sensors for measurement of phase volume fraction in two-phase pipelines," *IEEE Trans. Instrum. Meas.*, vol. 42, no. 3, pp. 726–729, Jun. 1993.
[31] S. I. M. Sheikh, E. E. Hassan, M. S. Iqbal, and H. Attia, "Novel solution for multi-phase semi-cylindrical capacitive sensors," *IEEE Access*, vol. 7, pp. 116342–116347, 2019.
[32] F. Reverter, X. Li, and G. C. M. Meijer, "Liquid-level measurement system based on a remote grounded capacitive sensor," *Sens. Actuators A, Phys.*, vol. 138, no. 1, pp. 1–8, Jul. 2007.
[33] J. R. Hanni and S. K. Venkata, "A novel helical electrode type capacitance level sensor for liquid level measurement," *Sens. Actuators A, Phys.*, vol. 315, Nov. 2020, Art. no. 112283.
[34] B. Jin, Z. Zhang, and H. Zhang, "Structure design and performance analysis of a coaxial cylindrical capacitive sensor for liquid-level measurement," *Sens. Actuators A, Phys.*, vol. 223, pp. 84–90, Mar. 2015.
[35] S. Upadhyay and A. Ratnoo, "Continuous-curvature path planning with obstacle avoidance using four parameter logistic curves," *IEEE Robot. Autom. Lett.*, vol. 1, no. 2, pp. 609–616, Jul. 2016.
[36] P. G. Gottschalk and J. R. Dunn, "The five-parameter logistic: A characterization and comparison with the four-parameter logistic," *Anal. Biochem.*, vol. 343, no. 1, pp. 54–65, Aug. 2005.
[37] K. H. Chon, S. Dash, and K. Ju, "Estimation of respiratory rate from photoplethysmogram data using time-frequency spectral estimation," *IEEE Trans. Biomed. Eng.*, vol. 56, no. 8, pp. 2054–2063, Aug. 2009.
[38] J. D. Davies, M. H. Senussi, and E. Mireles-Cabodevila, "Should a tidal volume of 6 mL/kg be used in all patients?" *Respiratory Care*, vol. 61, no. 6, pp. 774–790, Jun. 2016.

SANGHUN SHIN received the B.S. degree from Hanyang University, South Korea, in 2019, where he is currently pursuing the M.S. and Ph.D. degrees with the Mechanical Engineering Department. His research interests include physical sensors, soft actuators, smart manufacturing-based microsystems, and artificial intelligence.

GAHUI PARK is currently pursuing the B.S. degree with the Department of Electronics Convergence Engineering, Hanyang University, South Korea. Her research interests include sensors, microfabrication, 3D printing, and electronic circuits design.

WHOI-YUL KIM (Member, IEEE) received the Ph.D. degree in electrical engineering from Purdue University, West Lafayette, IN, USA, in 1989. From 1989 to 1994, he was an Assistant Professor at the University of Texas at Dallas. He joined Hanyang University, in 1994, where he is currently a Professor with the Department of Electronic Engineering. His research interests include health monitoring using mobile devices, visual surveillance, virtual devices, machine vision systems, advanced driver assistance systems, and 3D vision systems for sport and in-home appliances.

HONGYUN SO (Member, IEEE) received the Ph.D. degree in mechanical engineering from the University of California at Berkeley, in 2014. He joined Stanford University as a Postdoctoral Scholar with the Aeronautics and Astronautics Department, in 2015. He is currently an Assistant Professor with the Mechanical Engineering Department, Hanyang University. His research interests include design, modeling, and manufacturing of micro/nanosystems, harsh-environment sensors, and mechanical issues related to heat transfer and fluid mechanics.